

A comprehensive comparison of different MPPT techniques for photovoltaic systems

Hegazy Rezk^{a,*}, Ali M. Eltamaly^{b,c}

^a *Electrical Engineering Dept., Faculty of Engineering, Minia University, Minia, Egypt*

^b *Sustainable Energy Technologies Center, King Saud University, Riyadh, Saudi Arabia*

^c *Electric Engineering Department, Al-Mansoura University, Egypt*

Received 1 April 2014; received in revised form 1 November 2014; accepted 8 November 2014

Communicated by: Associate Editor Igor Tyukhov

Abstract

This paper aimed to study the behavior of different maximum power point tracking (MPPT) techniques applied to PV systems. In this work, techniques such as hill climbing (HC), incremental conductance (INC), perturb-and-observe (P&O), and fuzzy logic controller (FLC) are assessed. A model of PV module and DC/DC boost converter with the different techniques of MPPTs was simulated using PSIM and Simulink software. Co-simulation between PSIM and Simulink software packages is used to establish FLC MPPT technique. The co-simulation is done to take advantage of each program to handle certain part of the system. The response of the different MPPT techniques is evaluated in rapidly changing weather conditions. The results indicate that, FLC performed best among compared MPPT techniques followed by P&O, INC, and, HC MPPT techniques in both dynamic response and steady-state in most of the normal operating range.

© 2014 Elsevier Ltd. All rights reserved.

Keywords: Maximum power point trackers; Incremental conductance; Perturb-and-observe; Hill climbing; Fuzzy logic; MPPT

1. Introduction

Renewable energy sources such as photovoltaic (PV) power play a crucial role in electric power generation, and become essential these days due to shortage and environmental impacts of conventional fuels. In the future, PV energy will gain more importance due to the shortage of fossil fuels and their environmental effects. More than 45% of necessary energy in the world will be generated by PV arrays (Faranda et al., 2008). Unfortunately, PV generation systems have two major problems: the conversion

efficiency of electric power generation is low, and the amount of electric power generated by solar arrays changes continuously with weather conditions (Berrera et al., 2009; Sreekanth and Raglend, 2012). Moreover, because of non-linear $I-V$ and $P-V$ characteristics of PV systems, their output power is always changing with weather conditions, i.e., solar radiation, atmospheric temperature and also nature of load connected (Fangrui et al., 2008; Emad and Masahito, 2010). Maximum power point tracking (MPPT) is essential as there is a probable mismatch between the load characteristics and the maximum power points (MPPs) of the PV module in order to ensure optimal utilization of solar cells (Xiao and Dunford, 2004; Ashish et al., 2007). Using of MPPT leads to reduce the cost of energy generated by PV panels (Hohm and Ropp, 2000). In recent

* Corresponding author.

E-mail addresses: hegazy.hussien@mu.edu.eg (H. Rezk), eltamaly@ksu.edu.sa (A.M. Eltamaly).

years, a large number of techniques have been proposed for tracking the MPP of PV systems. There are many techniques available in the literature such as fractional open-circuit voltage and short-circuit current (Fangrui et al., 2008), the Artificial Neural Network (ANN) technique (El Sayed, 2013), and the fuzzy logic control (Eltamaly, 2010; Eltamaly et al., 2010). Also, it was demonstrated in Ibrahim and Houssiny (1999) technique to track the maximum power using look-up table in the microcomputer. Another common approach is to use the array power as the feedback. The popular tracking methods based on this approach are widely adopted in PV power systems (Faranda et al., 2008) which include but not limited to, perturb and observe method (P&O) (Koutroulis et al., 2001; Ioan and Marcel, 2013), the incremental conductance method (INC) (Xiao and Dunford, 2004; Esham and Chapman, 2007) and the hill climbing method (HC). These techniques are widely applied in the MPPT controllers due to their simplicity and easy implementation. Several different MPPT methods have been proposed, but there has been no comprehensive comparison between different techniques and their tracking efficiencies under varying weather conditions. The objective of this work was to bridge this gap. In this work, the attention will be focused on simulation comparison study between these widely applied MPPT techniques, considering solar radiation variation in order to understand which technique has the best performance in fast changing weather conditions.

This paper is organized as follows; section II describes the PV system modeling, illustrates basic operation principles for HC, INC, P&O and FLC techniques respectively. Simulation results, analysis and discussion are illustrated in Section 3. Finally, conclusions are given in Section 4.

2. PV system modeling

The solar PV generation system consists of a PV module, DC/DC boost converter and a battery as shown in Fig. 1. Radiation (R) is incident on the PV module. It generates a voltage (V) and current (I). The temperature of the module is measured at T . The negative terminal of the battery and the module are connected and are also connected to ground. The simulation of the PV system has been

carried out using MPPT based on different techniques; HC, INC, P&O and, FLC. The system submodels are explained in the following sections:

2.1. PV solar module

The PV module used in this study consists of 36 polycrystalline silicon solar cells electrically configured as two series strings of 18 cells each. Its main electrical specifications are shown in Table 1. The equivalent circuit model for a PV module is addressed in Khaehintung et al. (2006), Abouobaida and Cherkaoui (2012), Emad and Masahito (2011), Christy et al. (2014), Gokmen et al. (2013).

2.2. DC/DC boost converter

According to maximum power transfer theory, maximum power is being transferred from source to load when source impedance is equal to the load impedance (load matching). The load matching can be done by adjusting the duty cycle of the DC/DC converter. The duty cycle is the ratio between the switching on time of switch to the switching period. In order to track MPP the converter must be operated with duty cycle corresponding to it. With varying atmospheric conditions the duty cycle of the DC/DC converter has to be adjusted to extract maximum power from PV module (RezaReisi et al., 2013). There are several architectures of DC/DC conversion circuits which can be used for this purpose. In the present work the boost configuration is chosen due to its wide spread use and high reliability with respect to other more complex configurations (Berrera et al., 2009). The complete power device scheme is shown in Fig. 1. The diode D_1 is provided to protect the PV module against negative current which could damage it. C_1 placed at boost input to limit the high frequency harmonic components (Berrera et al., 2009).

2.3. MPPT techniques

In this work, four MPPT techniques have been selected for the purpose of comparison; hill climbing (HC), incre-

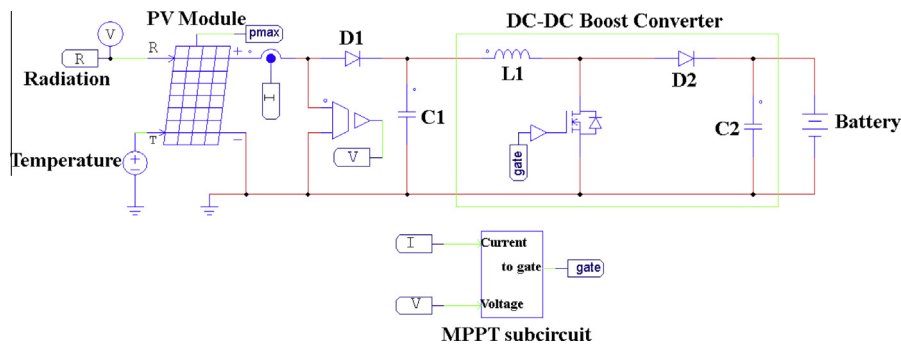


Fig. 1. Block diagram of a general PV system.

Table 1
The electrical specifications of MSX-60 PV module.

Maximum power (P_{\max})	60 W
Voltage @ P_{\max} (V_{mp})	17.1 V
Current @ P_{\max} (I_{mp})	3.5 A
Short-circuit current (I_{sc})	3.8 A
Open-circuit voltage (V_{oc})	21.1 V

mental conductance (INC), perturb and observe (P&O) and fuzzy logic controller (FLC).

(1) Hill climbing (HC) technique

The advantage of the hill climbing MPPT technique is its simplicity. It uses the duty cycle of boost converter as the judging parameter when the task of the maximum power point tracking is implemented. When the condition $dP/dD = 0$ is accomplished, it represents that the maximum power point has been tracked (Xiao and Dunford, 2004). The flow diagram of the HC algorithm is shown in Fig. 2. The duty cycle in every sampling period is determined by the comparison of the power at present time and previous time. If the incremental power $dP > 0$, the

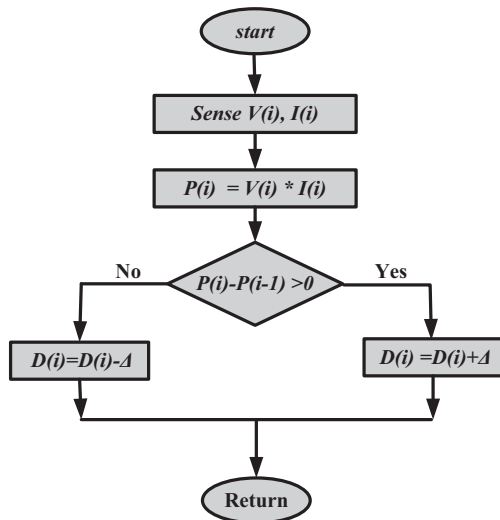


Fig. 2. State flow chart of HC MPPT technique.

duty cycle should be increased in order to make $dD > 0$. If $dP < 0$, the duty cycle is then reduced to make $dD < 0$. The main problem associated with this technique is because of the tradeoff between the stability of the system in constant radiation period and lack of fast response in rapidly changing radiation. The constant radiation period needs very small value of change in duty cycle, ΔD to prevent high oscillation of power around the maximum power point which reduces the energy captured from PV. On the other hand, the rapidly changing radiation needs higher value of duty cycle for fast tracking the maximum power. The flowchart of this technique is shown in Fig. 2. This technique has been simulated in the PSIM software package as shown in Fig. 3.

(2) Incremental conductance (INC) technique

Among all the MPPT strategies, the incremental conductance technique is widely used due to the high tracking accuracy at steady state and good adaptability to the rapidly changing atmospheric conditions (Fangrui et al., 2008). This technique employs the slope of the PV array power characteristics to track MPP. The slope of the PV array power curve is zero at the MPP, positive for values of output voltage smaller than the voltage at MPP, and negative for values of the output voltage greater than the voltage at MPP. The derivative of the PV module power is given as in (1), and the resultant equation for the error e is as in (2) (Abouobaida and Cherkaoui, 2012; Emad and Masahito, 2011; Chen et al., 2014).

$$\frac{dP}{dV} = \frac{d(V \times I)}{dV} = I + V \frac{dI}{dV} = 0 \quad (1)$$

$$\text{Also, } \frac{dI}{dV} + \frac{I}{V} = \frac{I(i) - I(i-1)}{V(i) - V(i-1)} + \frac{I(i)}{V(i)} = 0$$

$$e = \frac{I(i) - I(i-1)}{V(i) - V(i-1)} + \frac{I(i)}{V(i)} \quad (2)$$

Therefore tracking the MPP requires the following procedure as shown in Fig. 4. It can be implemented by a simple discrete integrator with the error signal e as the input, and a scaling factor k . The function of the scaling factor k is to adapt the error signal e to a proper range before the integral compensator. As the operating point

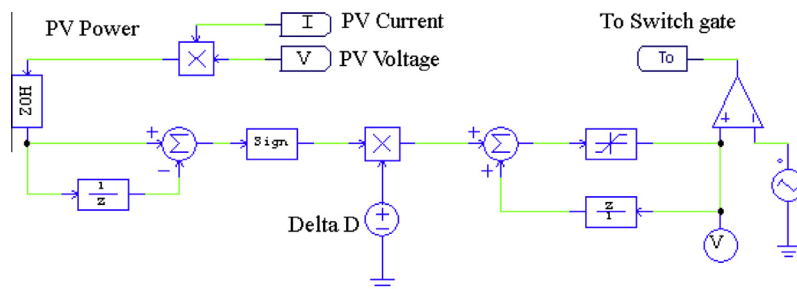


Fig. 3. Implementation of HC MPPT control technique using PSIM software.

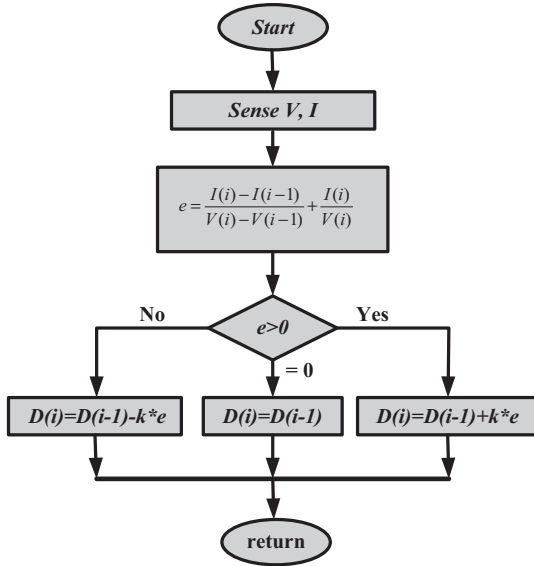


Fig. 4. State-flow chart of INC MPPT technique.

approaches the MPP, the error signal e becomes smaller, resulting in an adaptive and smooth tracking (Abouobaida and Cherkaoui, 2012).

To improve, both, the MPPT speed and accuracy simultaneously a modified dynamic change in step size for INC is introduced (Fangrui et al., 2008). This technique improves the performance of INC technique but at a cost of increased complexity of the control system.

The flow chart for INC technique is shown in Fig. 4 which was simulated in the PSIM software package as shown in Fig. 5.

(3) Perturb and observe (P&O) technique

P&O is the most frequently used technique to track the maximum power due to its simple structure (Ioan and Marcel, 2013). This technique operates by periodically perturbing the PV module terminal voltage and comparing the PV output power with that of the previous perturbation cycle (Faranda et al., 2008). As shown in Fig. 6 if the PV module operating voltage changes and power increases the control system moves the operating point in that direction; otherwise the operating point is moved in the opposite direction. The flowchart of this technique is shown in Fig. 6. PSIM software package has been used to simulate this technique as shown in Fig. 7. A common problem in

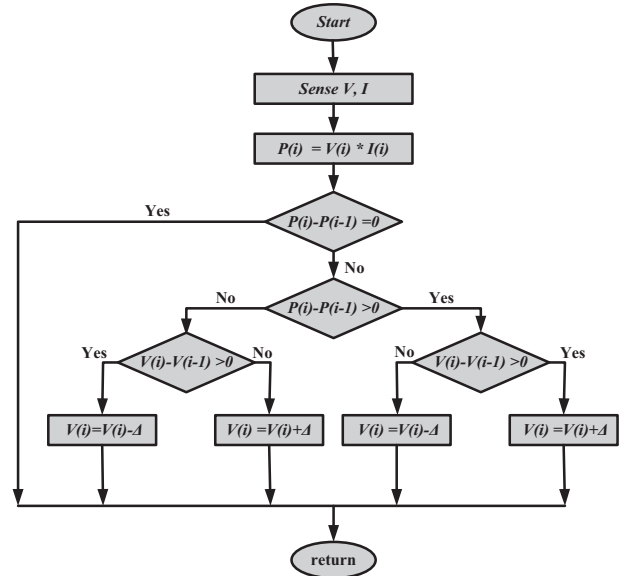


Fig. 6. State flowchart of P&O MPPT technique.

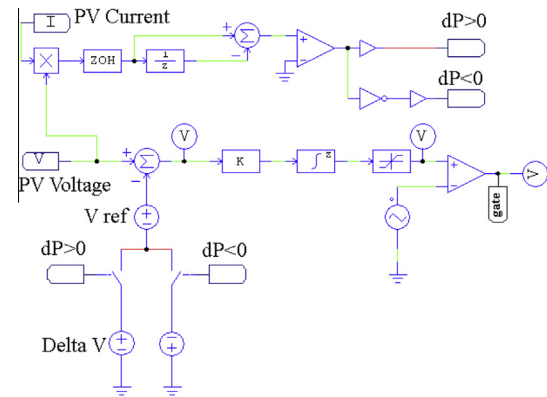


Fig. 7. P&O MPPT control technique using PSIM software.

this technique is that the PV module terminal voltage is perturbed every MPPT cycle; therefore when the MPP is reached, the output power oscillates around the maximum, resulting in power loss in the PV system. To remedy this problem, a modified P&O technique has been introduced in Al-Diab and Sourkounis (2010) by multiplying the change in the duty cycle by dynamic constant depending on the previous change in the extracted power as shown in (1). Another technique (Amrouche et al., 2007) used

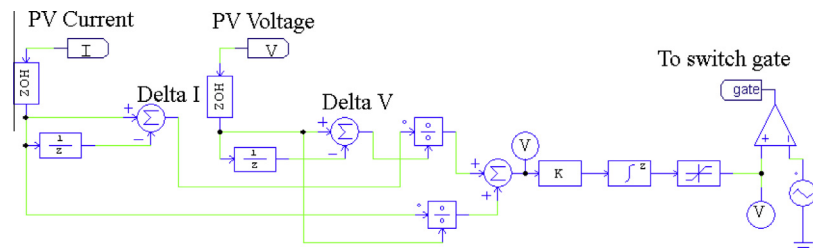


Fig. 5. INC MPPT control technique using PSIM software.

ANN to predict this multiplying constant. These techniques increase the complexity of the system and may cause more oscillations in stable weather conditions.

(4) Fuzzy logic controller (FLC) technique for PV MPPT

FLC has been introduced in many researches as in Gounden et al. (2009), Ben Salah et al. (2008), Altasa and Sharaf (2008), Khaehintung et al. (2004), Karlis et al. (2007), Veerachary et al. (2003), Rajesh and Mabel (2014) to force the PV to work around MPP. FLCs have the advantages of working with imprecise inputs, not needing an accurate mathematical model, and handling nonlinearity. The details of using FLC in MPPT of PV system are shown in Eltamaly (2010). The error signal can be calculated as shown in (3). The value of ΔE is calculated as shown in (4). The model of the proposed system has been simulated in co-simulation between PSIM and Simulink software packages. The idea behind using co-simulation is the easy simulation of FLC in Simulink and power circuit in PSIM.

$$E(n) = \frac{P(i) - p(i-1)}{V(i) - V(i-1)} \quad (3)$$

$$\Delta E(i) = E(i) - E(i-1) \quad (4)$$

The detailed logic, theory and implementation of this model can be found in Eltamaly (2010) and Eltamaly et al. (2010). The output power from the PV system and the voltage are used to determine the E and ΔE based on (4) and (5). The inputs to a FLC are usually E and ΔE . The range of E and ΔE are fixed judiciously based on trial and error. These variables are expressed in terms of linguistic variables or labels such as PB (Positive Big), PM (Positive Medium), PS (Positive Small), ZE (Zero), NS (Negative Small), NM (Negative Medium), NB (Negative Big) using basic fuzzy subset. Each of these acronyms is described by a mathematical membership functions, MF as shown in Fig. 8. Once E and ΔE calculated and converted to the linguistic variables based on MF, the FLC

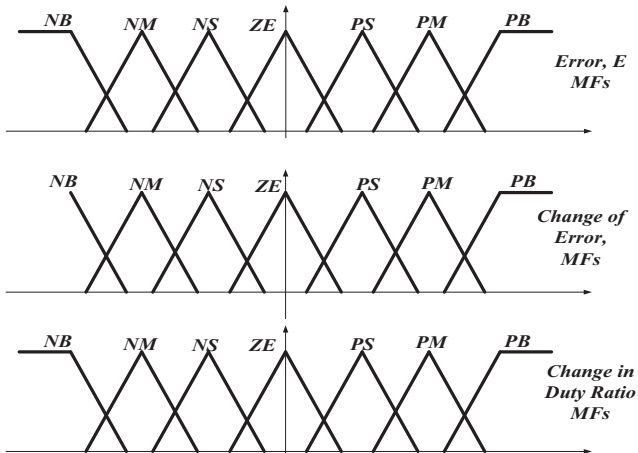


Fig. 8. A fuzzy system with two inputs, 1 output and 7 MFs each.

Table 2
Rules for a fuzzy system.

E	ΔE						
	NB	NM	NS	ZE	PS	PM	PB
NB	NB	NB	NB	NB	NM	NS	ZE
NM	NB	NB	NB	NM	NS	ZE	PS
NS	NB	NB	NM	NS	ZE	PS	PM
ZE	NB	NM	NS	ZE	PS	PM	PB
PS	NM	NS	ZE	PS	PM	PB	PB
PM	NS	ZE	PS	PM	PB	PB	PB
PB	ZE	PS	PM	PB	PB	PB	PB

output, which is typically a change in duty cycle, ΔD of the power converter, can be looked up in a rule base given in Table 2. A triangular membership function can be used for both inputs and output variables, as it can easily be implemented on the digital control system. The linguistic variables assigned to ΔD for the different combinations of E and ΔE are based on the power converter being used and also on the knowledge of the user.

These linguistic variables of input and output MFs are then compared to a set of pre-designed values during aggregation stage. The proper choice of If-then rules or fuzzy inference is essential for the appropriate response of the FLC system. The inference used in this work is tabulated in Table 2. Some researches proportionate these variables to only five fuzzy subset functions as in (Eltamaly et al., 2010). Table 2 can be translated into 49 fuzzy rules or IF-THEN rules to describe the knowledge of control as follows:

R_{25} : If E is NM and ΔE is PS then ΔD is NS

R_{63} : If E is PM and ΔE is NS then ΔD is PS

...

R_{51} : If E is PS and ΔE is NB then ΔD is NM

Defuzzification is for converting the fuzzy subset of control form inference back to values. As the plant usually required a nonfuzzy value of control, a defuzzification stage is needed. Defuzzification for this system is the height method. The height method is both very simple and very fast method. The height defuzzification method in a system of rules formally given by (6):

$$\Delta D = \left(\sum_{k=1}^m c(k) * W_k \right) / \sum_{k=1}^n W_k \quad (5)$$

where ΔD = change of duty cycle; $c(k)$ = peak value of each output; W_k = height of rule k .

In the defuzzification stage, FLC output is converted from a linguistic variable to a numerical variable. This provides an analog signal which is ΔD of the boost converter. This value is subtracted from previous value of D to get its new value.

PSIM model showing the calculating E and ΔE and the inputs to Simulink is shown in Fig. 9. The simulation model showing the output signal from FLC in Simulink

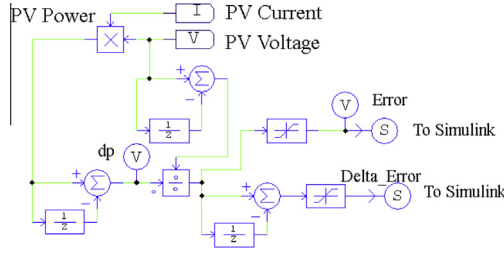


Fig. 9. PSIM model showing the calculating E and ΔE and the inputs to Simulink.

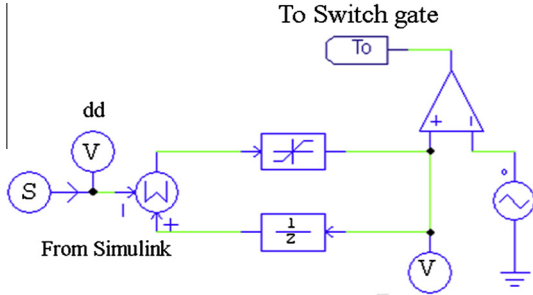


Fig. 10. Simulation model of output signal from FLC in Simulink to PSIM and the switching circuit.

to PSIM and the switching circuit that control the switch is shown in Fig. 10. The simulation model of the proposed system in Simulink is shown in Fig. 11, where SLINK1 is the name that used in Simulink for the input to PSIM part of simulation.

3. Analysis and discussion of the simulation results

The whole system shown in Fig. 1 has been simulated using co-simulation of PSIM and Simulink software packages. It consists of a 60 W solar PV module, a DC/DC boost converter operating at switching frequency of 30 kHz, an input inductance of 1 mH, an output capacitor of 47 μ F and a 24 V battery. Four MPPT techniques are implemented in simulation as a controller to study and compare the dynamic response of the PV system under rapidly radiation changes. All simulations are performed with step changes in solar radiation. Fig. 12 indicates the solar

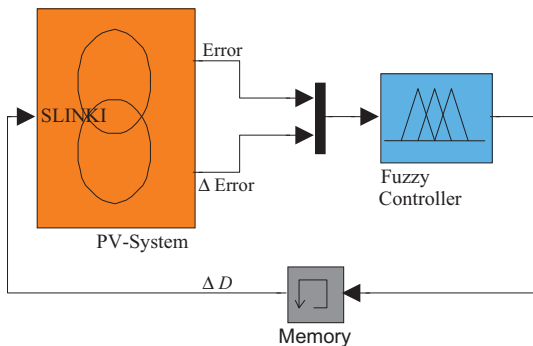


Fig. 11. Simulink simulation model of FLC MPPT.

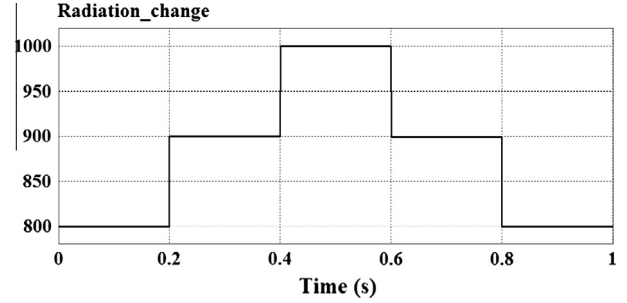


Fig. 12. Change in the solar radiation (W/m^2).

radiation profile used in simulation. A step change in radiation is applied to study the response of each technique during disturbance.

The MPPT techniques are compared in terms of dynamic response and the percentage reduction in energy. The percentage reduction in energy can be obtained from the following equation:

$$\%E_{\text{red}} = \frac{E_{\text{max}} - E}{E_{\text{max}}} * 100 \quad (6)$$

where E_{max} : the maximum energy that can be generated from PV; E : the generated energy generated from PV system during simulation time.

To compare the performance of the different MPPT techniques with change in duty cycle of boost converter, the simulations were performed under exactly the same conditions. The sampling time is the inverse of the sampling frequency. Sampling frequency defines the number of samples per second. The sampling time for the MPPT is chosen to be 0.01 sec. The duty cycle is therefore updated every 0.01 sec. The dynamic response of the PV module output power in case of using HC MPPT technique with different increment in the duty cycle, $\Delta D = 2\%$, 4% , 6% , 8% and 10% respectively. Figs. 13 and 14 shows the dynamic response of HC MPPT in starting and steady state respectively. It is clear from Fig. 13 that the starting time is inversely proportional to the incremental value of duty cycle ΔD . The maximum starting time to reach the maximum power for 800 W/m^2 radiation occurs at the lower value of ΔD ($\Delta D = 2\%$) which is about 0.16 sec, which does not have a

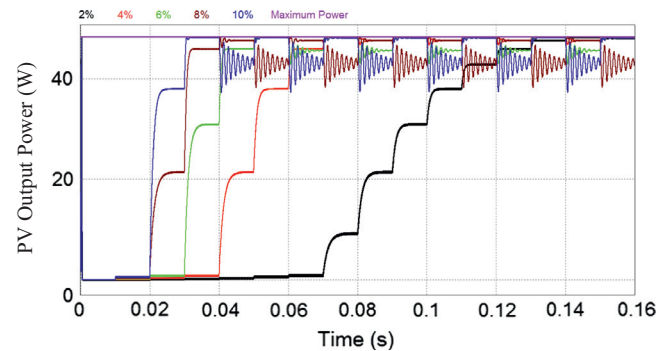


Fig. 13. Starting period of HC-MPPT for $\Delta D = 2\%$, 4% , 6% , 8% and 10% .

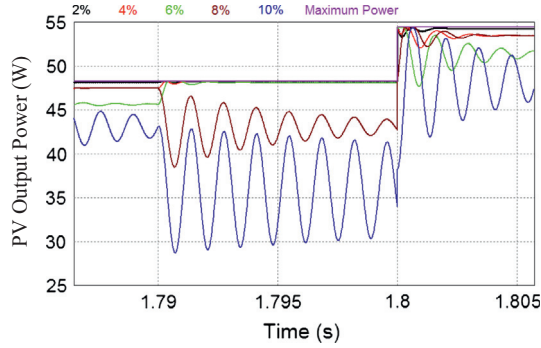


Fig. 14. Dynamic response of the PV module output power with HC-MPPT for $\Delta D = 2\%$, 4% , 6% , 8% and 10% .

serious effect on the performance of the PV system. The minimum starting time to reach the maximum power for 800 W/m^2 radiation occurs at the higher value of ΔD ($\Delta D = 10\%$) which is about 0.03 sec. This proves that the higher the ΔD the quicker will be tracking of the maximum power. Fig. 13 shows that the oscillation of the generated power is directly proportional to ΔD . It is clear from this technique that it has difficulty in providing good performance in both dynamic and steady-state response together because of the tradeoff between the steady state performance and transient stability. As seen in Fig. 14, in steady state (constant radiation) the better performance can be achieved with lower values of ΔD but the fast response in rapidly changing radiation can be achieved with higher values of ΔD . So, a smart compromising between the effects of ΔD on the operation of the HC-MPPT in steady state and transient stability should be considered.

The dynamic response of the PV module output power in case of using INC MPPT technique with different increment in the duty cycle, $\Delta D = 2\%$, 4% , 6% , 8% and 10% is shown in Fig. 15 (starting/transient) and Fig. 16 (steady state), respectively. It is clear from Fig. 15 that the starting time is inversely proportional to the incremental value of duty cycle ΔD . The maximum starting time to reach the maximum power for 800 W/m^2 radiation occurs at the lower value of ΔD which is about 0.15 sec, which does not have a serious effect on the performance of the PV system especially on low change in radiation. But, in case of

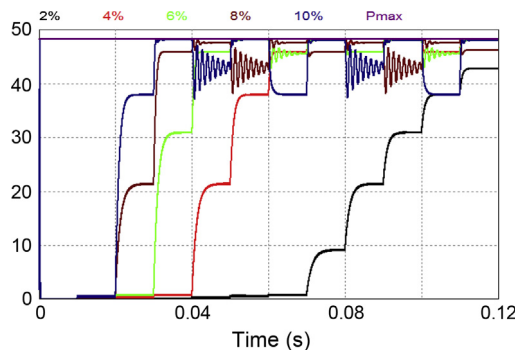


Fig. 15. Starting period of INC-MPPT for $\Delta D = 2\%$, 4% , 6% , 8% and 10% .

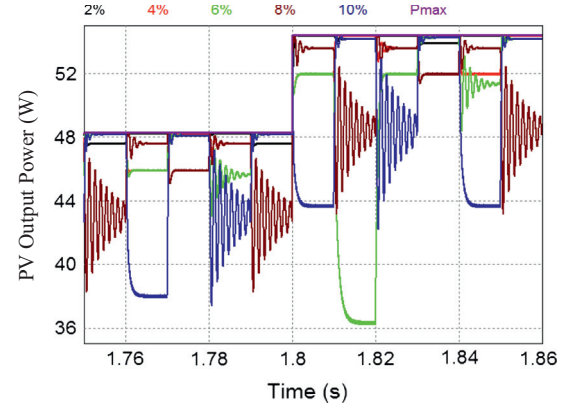


Fig. 16. Dynamic response of the PV module output power with INC-MPPT for $\Delta D = 2\%$, 4% , 6% , 8% and 10% .

fast change in radiation especially in tropical environment this MPPT will take longer time to follow the maximum power point which will reduce the energy captured from the system. This proves that the higher the ΔD the quick reach of the maximum power. Fig. 16 shows that the oscillation of the generated power is directly proportional to the ΔD . It is clear from this technique that it has difficulty in providing good performance in both dynamic and steady-state response together because of the tradeoff between the steady state performance and transient stability. It is clear that in steady state (constant radiation) the better performance can be achieved with lower values of ΔD but the fast response in rapidly changing radiation can be achieved with higher values of ΔD . Also, it is clear that INC technique has better performance than HC technique in both the transient and steady state response.

The dynamic response of the PV module output power in case of using P&O MPPT technique with different increment in the duty cycle, $\Delta D = 2\%$, 4% , 6% , 8% and 10% is shown in Fig. 17 (starting/transient) and Fig. 18 (steady state), respectively. The maximum starting time (about 0.16 sec) to reach the maximum power, at 800 W/m^2 radiation, occurs at the lower value of ΔD (2%). This proves that the higher the ΔD the quick reach of the maximum power.

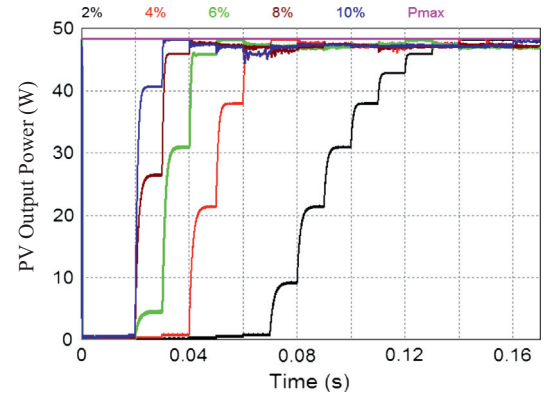


Fig. 17. Starting period of P&O-MPPT for $\Delta D = 2\%$, 4% , 6% , 8% and 10% .

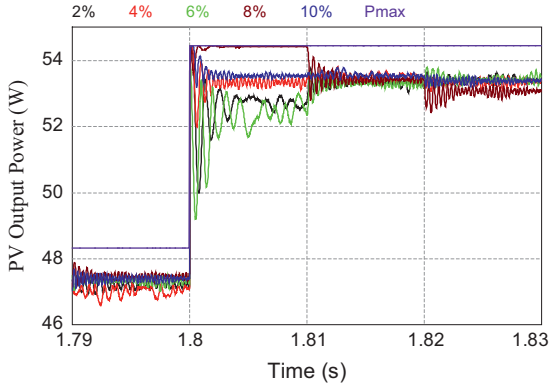


Fig. 18. Dynamic response of the PV module output power with P&O-MPPT for $\Delta D = 2\%$, 4% , 6% , 8% and 10% .

It is clear from results shown in Figs. 13–18 that the starting current for HC, INC, and P&O is almost the same for all values of ΔD . Fig. 18 shows that the oscillation of the generated power for P&O is almost constant with all values of ΔD . It is clear from the simulation results of this technique that it can work with almost same oscillation for all values of ΔD . So, high value of ΔD can be chosen for fast response in rapidly changing radiation and this value will not considerably affect the performance of steady state (constant radiation). Hence, with P&O technique it is possible to achieve the satisfactory performance in both transient and steady state which is its major benefit over HC and INC techniques.

The simulation of the FLC for MPPT has been carried out by co-simulation between PSIM and Simulink simulation packages as shown in Figs. 9–11. The motivation for using the co-simulation is that the PSIM is more effective and simple for power electronics PV module development and Simulink is better in handling fuzzy logic control. The simulation of FLC technique with different increment in the duty cycle, $\Delta D = 2\%$, 4% , 6% , 8% and 10% respectively was performed. Figs. 19 and 20 show the dynamic response of FLC MPPT technique in starting and steady state respectively. It is clear from Fig. 19 that the starting time is inversely proportional to the incremental value of duty cycle ΔD . The maximum starting time to reach the

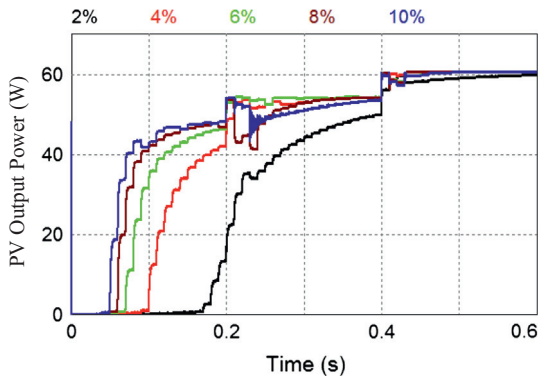


Fig. 19. Starting power of FLC-MPPT for $\Delta D = 2\%$, 4% , 6% , 8% and 10% .

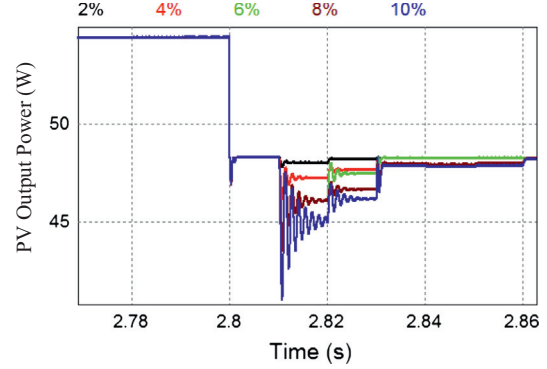


Fig. 20. Dynamic response of the PV module output power with FLC-MPPT for $\Delta D = 2\%$, 4% , 6% , 8% and 10% .

maximum power for 800 W/m^2 radiation occurs at the lower value of ΔD which is about 0.6 sec. Fig. 20 shows that the oscillation of the generated power is directly proportional to the ΔD but for a very short time after the transient occurs, after that the oscillations with all values of ΔD are almost similar. It is clear from the simulation results of this technique that it has better performance than other techniques in both dynamic and steady-state response together because of the dynamic change of the ΔD depending on the situation required.

Fig. 21 shows three traces showing the performance of FLC-MPPT in starting period for 2%, 4%, 6%, 8% and 10% as a maximum value of ΔD . In the upper trace of this figure, the power generated with respect to the maximum power. The middle trace of Fig. 21 shows the variation of ΔD for each case. The lower trace shows the duty cycle during starting period. It is clear from this figure that the starting time is inversely proportional to the maximum value of the duty cycle. Note that the value of ΔD becomes the same for all values of maximum allowable value of ΔD after the starting period and any sudden change in the radiation which prove that the value of maximum allowable ΔD affects only in the transient periods.

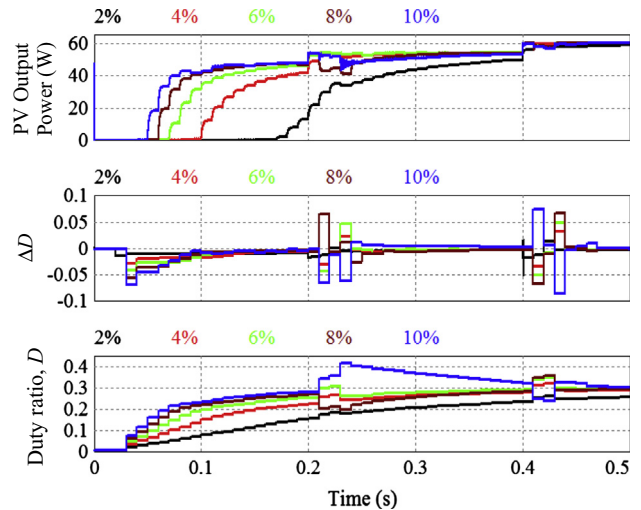


Fig. 21. The performance of FLC-MPPT in starting period for 2%, 4%, 6%, 8% and 10% as a maximum value of ΔD .

Fig. 22 shows three traces showing the performance of FLC–MPPT in normal operating period for 2%, 4%, 6%, 8% and 10% as a maximum allowable value of ΔD . In the upper trace of this figure, the power generated with respect to the maximum power. In the middle trace of Fig. 22 it shows the variation of ΔD for each case. The lower trace shows the duty cycle in starting period. It is clear from this figure that the starting time is inversely proportional to the maximum value of the duty cycle. Also it is notable that the value of ΔD becomes the same for all values of maximum allowable value of ΔD after the normal operating period and any sudden change in the radiation which prove that the value of maximum allowable ΔD affects only in the transient periods.

Fig. 23 shows the variation of the generated power of PV in the upper trace and duty cycle, D in the lower trace during starting period for HC, INC, P&O, and FLC MPPT techniques. The best value for ΔD in each technique has been chosen for each technique as has been discussed before. So, the change in duty cycle, ΔD is chosen to be 2% for HC, INC, and P&O and 10% for FLC technique. It is clear from this figure that there is no much difference on starting time between FLC and the other MPPT techniques under study, where all of them reach the maximum power within 0.2 sec. approximately. The slowest technique is FLC MPPT technique and the fastest technique is the INC technique. The limited difference in starting time does not affect the generated energy considerably.

Fig. 24 shows the variation of the generated power of PV in the upper trace and duty cycle, D in the lower trace during rapid change of radiation period for HC, INC, P&O, and FLC MPPT techniques. The best value for ΔD in each technique has been chosen for each technique as has been discussed before. So, the change in duty cycle, ΔD is chosen to be 2% for HC, INC, and P&O and 10% for FLC technique. It is clear from this figure that the fuzzy controller technique has the best tracking for the maximum

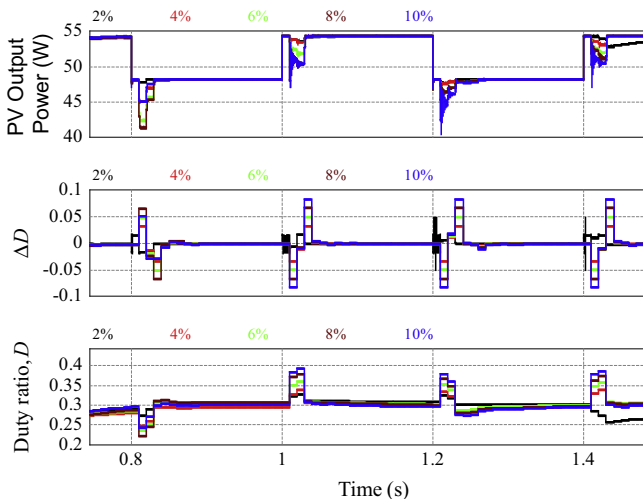


Fig. 22. Dynamic response of the PV module of output power, ΔD , D with FLC–MPPT for $\Delta D = 2\%$, 4% , 6% , 8% and 10% .

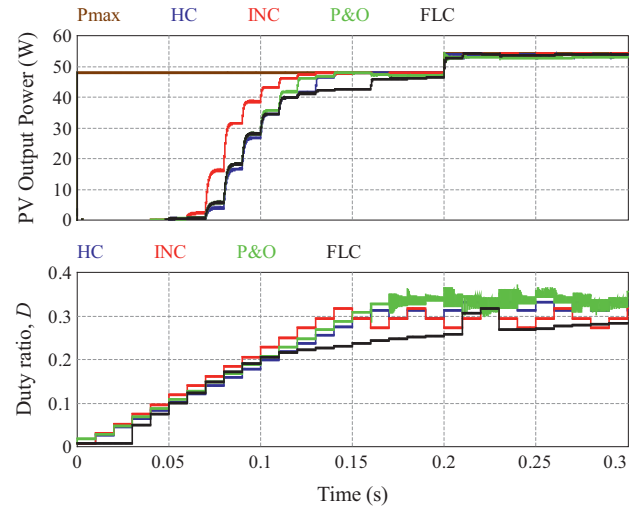


Fig. 23. The variation of the generated power of PV and duty cycle, D respectively during starting period for all techniques under study.

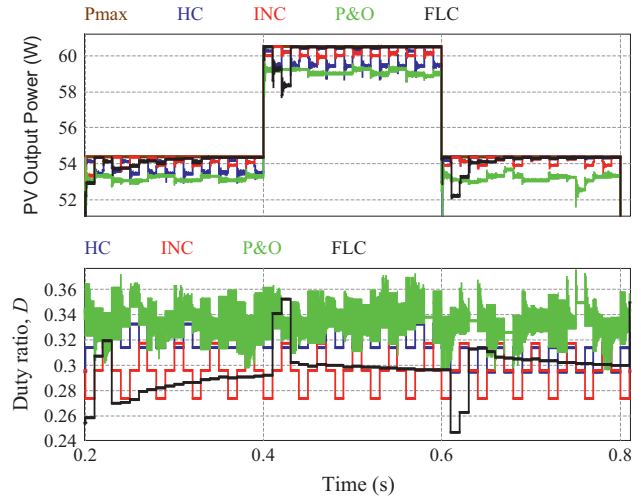


Fig. 24. The variation of the generated power of PV and duty cycle, D for all techniques under study.

power than the other techniques. Also, it can be observed that oscillation around maximum power is limited with FLC technique followed by P&O, INC, and HC techniques.

Fig. 25 shows the starting time required for each MPPT technique under study to reach the maximum power corresponding to 1 kW/m^2 solar radiation along with the maximum allowable change in duty cycle ΔD . It is clear from this figure that the starting time is inversely proportional to the allowable change in duty cycle ΔD in all MPPT techniques under study. Also, it is clear from this figure that the starting time variations for HC, INC and P&O techniques are almost the same and are shorter than the time associated with the FLC technique. So, HC, INC and P&O techniques are better than FLC with respect to the starting time.

Fig. 26 shows the percentage reduction of energy along with the maximum allowable change in the duty cycle, ΔD

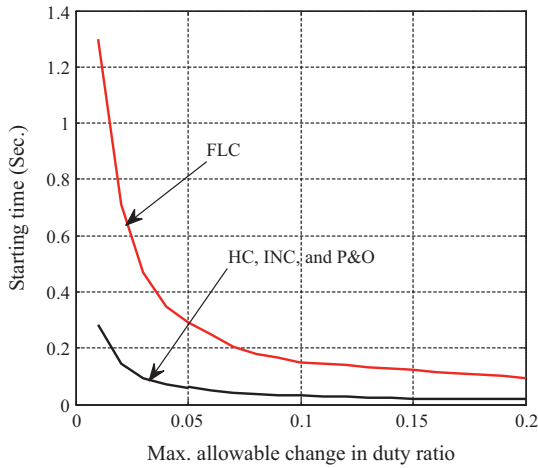


Fig. 25. The starting time required for each MPPT technique under study.

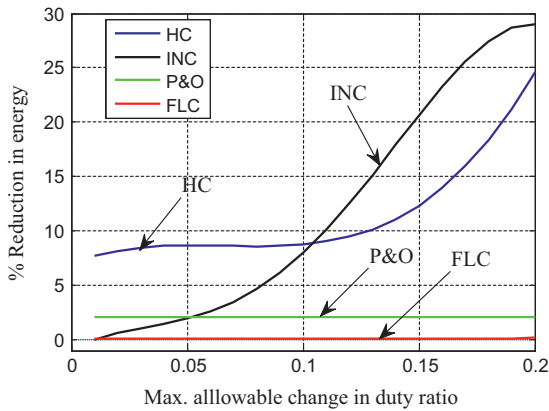


Fig. 26. The percentage reduction of energy along with the maximum allowable change in the duty cycle, ΔD .

for four MPPT techniques under study. These curves have been drawn for the simulation of normal operating range without rapid change in radiation to ideally compare the generated energy. It is clear that INC technique has the lower percentage reduction in the generated energy compared to the P&O and HC in the range of maximum allowable change in duty cycle for range $D < 5\%$. However, the FLC technique has the lower percentage reduction in the generated energy compared to other MPPT under study in all the range of maximum allowable change in duty ratio which makes it the best technique. But, FLC is the worst starting time compared to the other techniques under study. But, starting time has lower importance than the percentage reduction in the generated energy.

From the simulation results depicted in Figs. 25 and 26 MPPT techniques under study can be ranked from best to worst as: FLC, P&O, INC, and HC.

4. Conclusions

In this paper, four MPPT techniques have been compared on the basis of, both, transient and steady-state

response of PV system. The simulation results show that, FLC technique has the lower percentage reduction in the generated energy compared to all the other techniques under study in the entire range of duty cycle. It is followed by the INC technique, which has the lower percentage reduction in the generated energy than the P&O and HC for change in duty cycle in the range lower than 5%.

On the transient performance front, FLC performed worst, with highest settling time compared to the other techniques under study. On the basis of transient performance, the rank of the MPPT techniques under study is arranged from best to worst as follows: FLC, P&O, INC, and HC. Nevertheless, settling time has lower importance than the percentage reduction in the generated energy.

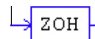
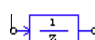




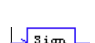
To summarize, when overall performance compared, the FLC and P&O are superior with respect to other MPPT techniques as they can effectively improve the tracking speed and minimize steady state error simultaneously.

Acknowledgments

The authors acknowledge the College of Engineering Research Center and Deanship of Scientific Research at King Saud University in Riyadh, Saudi Arabia, for the financial support to carry out the research work reported in this paper.

Appendix A

Description of PSIM blocks used in this paper

-  Zero-order hold (the ZOH samples the input at the beginning of a clock cycle, and holds the sampled value until the next clock cycle)
-  Unit delay block (a unit delay block delays the input by one sampling period)
-  Comparator (the output of a comparator is high (value = 1) when the non-inverting input is higher than the inverting input. When the positive input is lower, the output is zero. If the two inputs are equal, the output is undefined and it will keep the previous value)
-  NOT gate (the output is the inversion of the input logic signal)
-  On-off switch controller (the on-off switch controller interfaces between the control circuit and the power circuit)
-  Simple bidirectional switch (a simple switch conducts current in both directions. It is on when the gating is high, and is off when the gating is low)
-  Sign function block (the output of the sign function block is the sign of the input. When the input is positive, the output is 1. When the input is 0, the output is 0. When the input is negative, the output is -1)

References

- Abouobaida, H., Cherkaoui, M., 2012. Comparative study of maximum power point trackers for fast changing environmental conditions. In: *Multimedia Computing and Systems (ICMCS)*, International Conference, 10–12 May 2012, pp. 1131–1136.
- Al-Diab, A., Sourkounis, C., 2010. Variable step size P&O MPPT algorithm for PV systems. In: *Optimization of Electrical and Electronic Equipment (OPTIM)*, 12th IEEE International Conference, pp. 1097–1102.
- Altasa, I.H., Sharaf, A.M., 2008. A novel maximum power fuzzy logic controller for photovoltaic solar energy systems. *Renew. Energy* 33, 388–399.
- Amrouche, B., Belhamel, M., Guessoum, A., 2007. Artificial intelligence based P&O MPPT method for photovoltaic systems. *Revue des Energies Renouvelables ICRESD-07 Tlemcen*, 11–16.
- Ashish, P., Nivedita, D., Ashok, K.M., 2007. Comparison of various MPPT algorithms for cost reduction. *IEEE Trans. Power Electron.* 22 (2), 698–700.
- Ben Salah, C., Chaabene, M., Ben Ammara, M., 2008. Multi-criteria fuzzy algorithm for energy management of a domestic photovoltaic panel. *Renew. Energy* 33, 993–1001.
- Berrera, M., Dolara, A., Leva, S., 2009. Experimental test of seven widely adopted MPPT algorithms. In: *IEEE Bucharest Power Tech Conference*, June 28th – July 2nd, Bucharest, Romania.
- Chen, Y.-T., Lai, Z.-H., Liang, R.-H., 2014. A novel auto-scaling variable step-size MPPT method for a PV system. *Sol. Energy* 102, 247–256.
- Christy, J.S., Raj, M., Jeyakumar, A.E., 2014. A two stage successive estimation based maximum power point tracking technique for photovoltaic modules. *Sol. Energy* 103, 43–61.
- Eltamaly, A.M., 2010. Modeling of fuzzy logic controller for photovoltaic maximum power point tracker. In: *Solar Future 2010 Conf. Proc.*, Istanbul, Turkey, February, pp. 4–9.
- Eltamaly, A.M., Alolah, A.I., Abdulghany, M.Y., 2010. Digital implementation of general purpose fuzzy logic controller for photovoltaic maximum power point tracker. In: *Power Electronics Electrical Drives Automation and Motion (SPEEDAM)*, 2010 International Symposium on Digital Object Identifier, pp. 622–627.
- Emad, M.A., Masahito, S., 2010. Modified adaptive variable step-size MPPT based-on single current sensor. In: *TENCON 2010 – IEEE Region 10 Conference*, 21–24 November, pp. 1235–1240.
- Emad, M.A., Masahito, S., 2011. Stability study of variable step size incremental conductance/impedance MPPT for PV systems. In: *Power Electronics and ECCE Asia (ICPE & ECCE)*, 2011 IEEE 8th International Conference, May 30 2011 – June 3, pp. 386–392.
- El Sayed, M., 2013. Modeling and simulation of smart maximum power point tracker for photovoltaic system. *Minia J. Eng. Technol. (MJET)* 32 (1).
- Esrar, T., Chapman, P.L., 2007. Comparison of photovoltaic array maximum power point tracking techniques. *IEEE Trans. Energy Convers.* 22 (2), 439–449.
- Fangrui, L., Shanxu, D., Fei, L., Bangyin, L., Yong, K., 2008. A variable step size INC MPPT method for PV systems. *IEEE Trans. Ind. Electron.* 55 (7), 2622–2628.
- Faranda, R., Leva, S., Maugeri, V., 2008. MPPT techniques for PV systems: energetic and cost comparison. *Power and Energy Society General Meeting – Conversion and Delivery of Electrical Energy in the 21st Century*, 20–24 July, pp. 1–6.
- Gokmen, N., Karatepe, E., Ugranli, F., Silvestre, S., 2013. Voltage band based global MPPT controller for photovoltaic systems. *Sol. Energy* 98, 322–334.
- Gounden, N.A., Peter, Sabitha A., Nallandula, Himaja, Krithiga, S., 2009. Fuzzy logic controller with MPPT using line-commutated inverter for three-phase grid-connected photovoltaic systems. *Renew. Energy J.* 34, 909–915.
- Hohm, D.P., Ropp, M.E., 2000. Comparative study of maximum power point tracking algorithms using an experimental, programmable, maximum power point tracking test bed. In: *Photovoltaic Specialists Conference*, Anchorage, AK, pp. 1699–1702.
- Ibrahim, H.E., Houssiny, F.F., 1999. Microcomputer controlled buck regulator for maximum power point tracker for DC pumping system operates from photovoltaic system. In: *IEEE International Fuzzy Systems Conference*, August 22–25, vol. 1, pp. 406–411.
- Ioan, V.B., Marcel, I., 2013. Comparative analysis of the perturb-and-observe and incremental conductance MPPT methods. In: *8th International Symposium on Advanced Topics in Electrical Engineering*, May 23–25, Bucharest, Romania.
- Karlis, A.D., Kottas, T.L., Boutalis, Y.S., 2007. A novel maximum power point tracking method for PV systems using fuzzy cognitive networks (FCN). *Electr. Power Syst. Res.* 77 (3–4), 315–327.
- Khaehintung, N., Wangtong, T., Sirisuk, P., 2006. FPGA implementation of MPPT using variable step-size P&O algorithm for PV applications. In: *International Symposium on Digital Object Identifier*, ISCIT, pp. 212–215.
- Khaehintung, N., Pramotung, K., Tuvirat, B., Sirisuk, P., 2004. RISC microcontroller built-in fuzzy logic controller of maximum power point tracking for solar-powered light-flasher applications. In: *30th Annu. Conf. IEEE Ind. Electron. Soc.*, pp. 2673–2678.
- Koutroulis, E., Kalaitzakis, K., Voulgaris, N.C., 2001. Development of a microcontroller-based photovoltaic maximum power point tracking control system. *IEEE Trans. Power Electron.* 16, 46–54.
- Rajesh, R., Mabel, M.C., 2014. Efficiency analysis of a multi-fuzzy logic controller for the determination of operating points in a PV system. *Sol. Energy* 99, 77–87.
- RezaReisi, A., Moradi, M.H., Jamasb, S., 2013. Classification and comparison of maximum power point tracking techniques for photovoltaic system: a review. *Renew. Sustain. Energy Rev.* 19, 433–443.
- Sreekanth, S., Raglend, I.J., 2012. A comparative and analytical study of various incremental algorithms applied in solar cell. In: *International Conference on Computing, Electronics and Electrical Technologies [ICCEET]*, 21–22 March, pp. 452–456.
- Veerachary, M., Senjyu, T., Uezato, K., 2003. Neural-network-based maximum-power-point tracking of coupled-inductor interleaved-boost converter-supplied PV system using fuzzy controller. *IEEE Trans. Ind. Electron.* 50 (4), 749–758.
- Xiao, W., Dunford, W.G., 2004. A modified adaptive hill climbing MPPT method for photovoltaic power systems. In: *35th Annual IEEE Power Electronics Specialist Conference*, vol. 3, pp. 1957–1963.